Biomaterials 30 (2009) 5178–5186

Contents lists available at ScienceDirect

Biomaterials

journal homepage: www.elsevier.com/locate/biomaterials

A paradigm for peptide vaccine delivery using viral epitopes encapsulated in degradable polymer hydrogel capsules

Siow-Feng Chong [a], Amy Sexton [b], Robert De Rose [b], Stephen J. Kent [b], Alexander N. Zelikin [a], Frank Caruso [a,*]

[a] Centre for Nanoscience and Nanotechnology, Department of Chemical and Biomolecular Engineering, The University of Melbourne, Parkville, Victoria 3010, Australia
[b] Department of Microbiology and Immunology, The University of Melbourne, Parkville, Victoria 3010, Australia

ARTICLE INFO

Article history:
Received 15 April 2009
Accepted 30 May 2009
Available online 9 July 2009

Keywords:
Layer-by-layer membrane
Drug delivery
Drug release
Cross-linking

ABSTRACT

We report on the use of degradable polymer capsules as carriers for the delivery of oligopeptide antigens to professional antigen presenting cells (APCs). To achieve encapsulation, oligopeptide sequences were covalently linked to a negatively charged carrier polymer via biodegradable linkages and the resulting conjugate was then adsorbed onto amine-functionalized silica particles. These peptide-coated particles were then used as templates for the layer-by-layer (LbL) deposition of thiolated poly(methacrylic acid) (PMA_{SH}) and poly(vinylpyrrolidone) (PVPON) multilayers. Removal of the silica core and disruption of the hydrogen bonding between PMA_{SH} and PVPON by altering the solution pH yielded disulfide-stabilized PMA capsules that retain the encapsulated cargo in an oxidative environment. In the presence of a natural reducing agent, glutathione, cleavage of the disulfide bonds causes release of the peptide from the capsules. The developed strategy provides control over peptide loading into polymer capsules and yields colloidally stable micron- and submicron-sized carriers with uniform size and peptide loading. The conjugation and encapsulation procedures were proven to be non-degrading to the peptide vaccines. The peptide-loaded capsules were successfully used to deliver their cargo to APCs and activate CD8 T lymphocytes in a non-human primate model of SIV infection *ex vivo*. The reported approach represents a novel paradigm in the delivery of peptide vaccines and other therapeutic agents.

1. Introduction

The successful treatment of disease relies on identifying drug targets and delivering safe and efficient therapeutics. Although there has been significant growth in the number of drug targets discovered in recent years, the development of targeted therapeutic delivery lags substantially behind. Vaccine delivery presents further hurdles since effective vaccination requires delivery of the vaccine to dendritic cells (DCs) [1,2], a small population of cells that coordinate effective immune responses. The use of oligopeptide sequences (immunogenic epitopes) has proven to be effective in eliciting cellular immune responses against various diseases [3–5], including models of HIV/AIDS [6], yet the application of oligopeptides as vaccines or immunotherapy agents is often hampered by their rapid degradation in the body [7]. To improve the efficiency of vaccines or therapeutics, conjugation and encapsulation techniques can be employed to prolong the blood residence time, protect the drug from degradation, target the agent to the required cell population, as well as shield other cells from any potential toxic effects of the agent [8–12]. A number of systems have been used as drug carriers, including polymers [8,9], microparticles [10], liposomes [11], lipid emulsions [12], and micelles [13]. While each of these platforms has its own advantages, no single system represents a complete solution for drug and vaccine delivery applications. A promising system for biomedical applications is based on colloidal capsules prepared by the layer-by-layer (LbL) adsorption of polymers onto sacrificial template particles [14,15]. This method provides control over the size of the capsules (from tens of nanometres [16–18] to several microns [19]), allows the use of biocompatible [20] and biodegradable [20,21] polymeric building blocks, and enables the engineering of capsules to respond to temperature [22], light [23–25] and pH [26]. Recent reports of LbL-assembled capsules have demonstrated their utility in applications ranging from drug delivery [27], targeting [28] and sensing [29,30] to the creation of microreactors [31,32] and artificial cells [33]. The success of these studies highlights the importance of the development of colloidally stable micron- to submicron-sized biodegradable capsules that can be reliably loaded with diverse

* Corresponding author. Tel.: +61 3 8344 3461; fax: +61 3 8344 4153.
E-mail address: fcaruso@unimelb.edu.au (F. Caruso).

0142-9612/$ – see front matter © 2009 Elsevier Ltd. All rights reserved.
doi:10.1016/j.biomaterials.2009.05.078

therapeutics and which specifically respond to intracellular triggers to induce cargo release.

Aimed at such a challenge, we have described capsules comprised of a synthetic polymer, poly(methacrylic acid), PMA, stabilized via biodegradable disulfide linkages [34]. The capsules are obtained via the sequential deposition of thiolated PMA (PMA_{SH}) and poly(vinylpyrrolidone) (PVPON) via hydrogen bonding onto the template silica particles (Scheme 1). Conversion of thiol groups into bridging disulfide linkages and removal of the core particles yields hollow capsules. The elevation of pH above the pK_a of PMA leads to the ionization of PMA and deconstruction of the hydrogen bonds between the layers, resulting in the release of PVPON from the capsule. The resulting single-component PMA hydrogel capsules are colloidally stable in a range of conditions, including the presence of blood serum proteins [35]. Furthermore, and of particular importance for biomedical applications, the capsules degrade in the presence of intracellular concentrations of a natural reducing agent, glutathione. We have used these capsules as carriers for globular proteins [36], single- and double-stranded DNA of varied length [37,38], and more recently, drug-loaded oil droplets [39]. However, the encapsulation of short oligopeptide sequences into PMA capsules (and other LbL-derived capsules) has remained a challenge due to their low molecular weight, which makes them freely permeable through the capsule wall.

Recently, we pioneered a method to use the PMA hydrogel capsules as carriers for viral epitopes for delivery into antigen presenting cells [35]. In the current paper, we characterize in detail this novel platform for vaccine delivery. We provide details of the method to achieve the encapsulation of a high payload of oligopeptide molecules into degradable micron- and submicron-sized PMA capsules and report the factors that govern the ability of the capsules to retain the cargo. Further, we present data on the release of an active therapeutic from the capsule in conditions of intracellular relevance, and on the capsules as carriers to deliver the payload to antigen presenting cells to elicit an immune response in an *ex vivo* model.

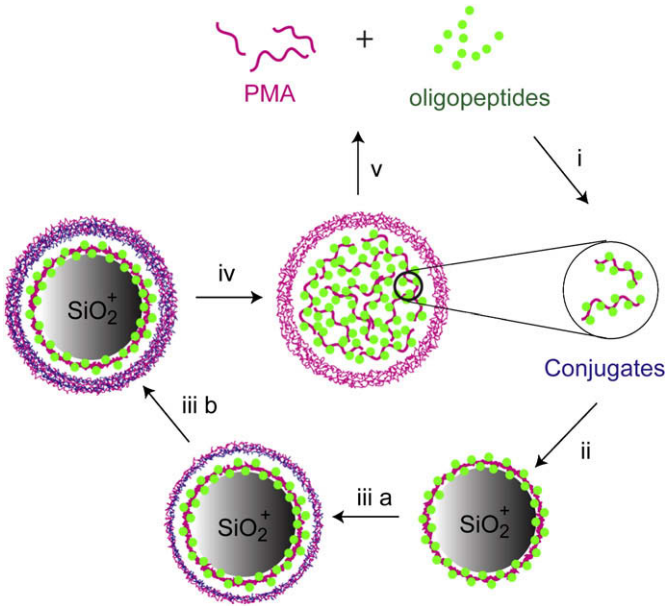

Scheme 1. Encapsulation of Cys-KP9 into degradable polymeric capsules: (i) Conjugation of oligopeptides to an anchoring PMA_{SH} polymer; (ii) adsorption of conjugates onto an amine-functionalized silica particle; (iii) assembly of a thin polymer film prepared via the alternating deposition of PVPON and PMA_{SH} and oxidation of PMA_{SH} thiol groups into bridging disulfide linkages; (iv) removal of the core particle to result in a stable polymer capsule; (v) degradation of the capsule, releasing Cys-KP9.

2. Materials and methods

2.1. Materials

SiO_2 particles of 0.5 and 1 μm diameter were purchased from MicroParticles GmbH as a 5 wt% suspension and were used as-received. Poly(methacrylic acid, sodium salt) (PMA), $M_w = 15$ kDa, was purchased from Polysciences (USA), and reduced L-glutathione (GSH), oxidized L-glutathione (GSSG), poly(vinylpyrrolidone) (PVPON), $M_w = 10$ kDa, 3-aminopropy-trimethoxysilane (APS), *N*-chloro-*p*-toluenesulfonamide sodium salt (chloramine T), cystamine dihydrochloride, cysteamine hydrochloride, *N*-(3-dimethylaminopropyl)-*N*′-ethylcarbodiimide (EDC), 5,5′-dithiobis-2-nitrobenzoic acid (Ellman's reagent), dithiothreitol (DTT), and *N*-hydroxysuccinimide (NHS) were purchased from Sigma–Aldrich and used as-received. Dimethylsulfoxide (DMF), ethylenediaminetetra acetic (EDTA), 2-(*N*-morpholine)ethane-sulfonic acid (MES), 3-morpholinopropane-1-sulfonic acid (MOPS), sodium hydrogen phosphate, sodium acetate, and 2-amino-2-hydroxymethyl-propane-1,3-diol (Tris) were purchased from Merck. Phosphate-buffered saline (PBS) was purchased from Invitrogen. The oligopeptide, CKKFGAEVVP-OH (Cys-KP9) and its *N*-terminus HiLyte Fluor™ 488 labeled analogue were purchased from AnaSpec Inc. and used without purification. High-purity water with a resistivity greater than 18 MΩ cm was obtained from an in-line Millipore RiOs/Origin system (MilliQ water).

2.2. Methods

Absorbance measurements were performed using an Agilent 8453 diode-array UV–Vis spectrophotometer. Flow cytometry was performed on a Becton Dickson FACS Calibur flow cytometer using an excitation wavelength of 488 nm and a CyFlow Space (Partec GmbH) flow cytometer with absolute volume counting. In each case at least 25 000 events were analyzed. Fluorescence measurements were conducted using a Fluorolog Horiba fluorescence spectrophotometer. Particles were imaged on an Olympus IX71 digital wide-field fluorescence microscope with a fluorescein filter cube and on a Leica time-correlated single-photon-counting confocal laser scanning microscope. The images were processed and volume rendered using Imaris v4.2 software (Bitplane AG). Zeta (ζ)-potential measurements were taken on a Malvern zetasizer.

2.3. Preparation of SiO_2^+ particles

A suspension of 1 μm diameter SiO_2 particles in 1 mL of ethanol was incubated with 250 μL of APS and 50 μL of 30% ammonia solution for 2 h. After this time, the particles were washed several times with ethanol and then MilliQ water (3×). The resulting particles had a ξ-potential of 33 ± 6 mV, as measured in sodium acetate buffer (10 mM; pH 4). SiO_2 particles of 0.5 μm diameter were functionalized in the same way, and the resulting particles had a ξ-potential of 34 ± 3 mV in sodium acetate buffer (10 mM; pH 4).

2.4. Preparation of PMA_{SH}

PMA samples with 5 and 12 mol% thiol groups were synthesized from PMA and cystamine dihydrochloride via carbodiimide coupling, as described previously [36]. The thiol content in the resulting polymer was characterized using Ellman's reagent and a cysteamine standard curve [40].

2.5. Reaction of PMA_{ER} with Cys-KP9

Cysteine-modified KP9 was conjugated to PMA through a disulfide linkage via thiol-disulfide exchange using a PMA_{SH} sample activated with Ellman's reagent. To achieve this, PMA_{SH} with 5 mol% thiol groups was dissolved in water at a concentration of 10 g L^{-1}. To this solution sodium borohydride was added to a final concentration of 1 M and the reaction mixture was incubated at room temperature for 2 h. Excess borohydride was neutralized by concentrated hydrochloric acid, the mixture was supplemented with K_2HPO_4 to a concentration of 0.1 M, and the pH was adjusted to 8 using HCl and NaOH. To this solution, excess Ellman's reagent was added, and the reaction was allowed to proceed for 30 min. The reaction mixture was purified via size exclusion chromatography using NAP-25 desalting columns (2×) and freeze-dried to obtain a light yellow powder of activated PMA_{SH} (PMA_{ER}).

A solution of PMA_{ER} (0.410 mg, 0.0871 μmol) in 475 μL of Tris–EDTA buffer (10 mM; pH 7.5) was combined with a solution of KP9 (0.348 μmol) in non-buffered water (25 μL), and the mixture was incubated overnight with constant mixing. The reaction mixture was purified using an NAP-25 desalting column (2×) and the conjugate was recovered by freeze-drying. Control samples were prepared under the same conditions using a commercially available pristine PMA sample (15 kDa).

For UV–Vis monitoring of the conjugation, solutions of PMA_{ER} and cysteine-modified KP9 in Tris–EDTA buffer (10 mM; pH 7.5) were combined directly in a spectrophotometric cuvette and spectra were recorded at specified time points.

2.6. Adsorption of PMA–KP9 conjugate onto colloidal particles

250 μg of SiO_2^+ particles were washed (3×) and dispersed with 25 μL of Tris–EDTA buffer (10 mM; pH 7.5). To this suspension was added 25 μL of the PMA–KP9 conjugate solution with varying concentrations (0–0.04 g L^{-1}), and adsorption was allowed to proceed for 15 min with constant shaking of the mixture. The resulting particles were washed (3×), and their fluorescence was quantified via flow cytometry.

2.7. Encapsulation of PMA–KP9 within polymer capsules

In a typical experiment, 250 μL of a 5 wt% suspension of SiO_2^+ particles were washed (3×) and dispersed into 125 μL with Tris–EDTA buffer (10 mM; pH 7.5). To this suspension was added 125 μL of the PMA–KP9 conjugate solution (1 g L^{-1}), and adsorption was allowed to proceed for 15 min with constant shaking of the mixture. The resulting particles with adsorbed PMA–KP9 were washed (3×) and redispersed into 250 μL of acetate buffer (20 mM; pH 4). The particles were finally used as substrates for the sequential deposition of PVPON and PMA_{SH}.

A stock solution of PVPON (100 g L^{-1}) was prepared using unbuffered water. Stock solutions of PMA_{SH} (50 g L^{-1}) were prepared using a 0.5 M solution of DTT in MOPS buffer (20 mM; pH 8) and incubated for at least 12 h prior to assembly of the multilayers to ensure the separation of the chains. All adsorption and washing steps were carried out from sodium acetate buffer (20 mM; pH 4). A suspension of template particles with the adsorbed PMA–KP9 conjugate was combined with an equal volume of a 2 g L^{-1} solution of PVPON and adsorption was allowed to proceed for 15 min with constant shaking. The particles were then washed via centrifugation/redispersion cycles (3×) using fresh buffer and finally dispersed in 250 μL for adsorption of the next polymer layer. The outlined procedure depicts the assembly of a single layer, and the process was repeated until the desired number of layers was assembled [34]. After completion of the multilayer build up, the particles were exposed to a 2.5 mM solution of chloramine T in MES buffer solution (20 mM; pH 6) for 1 min, followed by two washing cycles with MES buffer solution (10 mM; pH 6) [34]. The silica template particles were dissolved by treatment with an appropriate amount of aqueous HF, and the obtained capsules were washed via centrifugation/redispersion cycles using sodium acetate buffer (20 mM; pH 4). The washing cycles were repeated as necessary until the pH of the capsule suspension was identical to the pH of the washing buffer. The obtained capsules were stored as a suspension in pH 4 acetate buffer.

Prior to antigen presentation experiments, the capsules were equilibrated with PBS for at least 24–48 h to ensure removal of non-specifically bound and/or any leaked oligopeptide. This was verified via monitoring the fluorescence of the supernatant solutions.

2.8. Immunostimulatory activity of the capsule cargo

All macaque blood experiments were approved by the University of Melbourne animal ethics committee. Pigtail macaques expressed the MHC I allele, *Mane A*10*, which binds the 9 mer KP9 epitope from the SIV p27 capsid protein. Briefly, whole heparinised blood (100 μL) from a SIV_{mac251} infected *Mane-A*10*+ pigtail macaque was incubated at 37 °C (5% CO_2) with capsules or control samples. Co-stimulatory antibodies (anti-CD28 and CD49d, BD Biosciences) were also added (final concentration 1 μg mL^{-1}). After 3 h, brefeldin-A (Sigma) was added (final concentration of 10 μg mL^{-1}) to block secretion of expressed cytokines (except in the case of blood incubated with the capsule supernatant, in which brefeldin-A was added at the start of incubation). After a total of 6 h incubation, cells were surface stained for CD3 (clone SP34-2, BD Biosciences), CD8 (clone SK1, BD Biosciences) and KP9-specific T cells (using *Mane-A*10*/KP9 tetramer). Red blood cells were lysed with FACS lysing solution (BD Biosciences) and permeabilized with FACS Perm-2 solution (BD Biosciences) according to the manufacturer's instructions, before staining for intracellular IFN-γ (clone B27, BD Biosciences) and TNF-α accumulation (clone mAb11, BD Biosciences). Finally, cells were fixed with formaldehyde (1%) and acquired on a BD FACSCanto™ II flow cytometry system. Data were analyzed using Flowjo software (version 7.2). Cytokine expression from KP9-specific CD8 + T cells was analyzed by selecting CD3+ cells from the population of mononuclear cells, before gating on the required population from a CD8 versus *Mane-A*10*/KP9 tetramer plot.

3. Results and discussion

The encapsulation of drugs and reagents into multilayered polymer capsules has been achieved via two main pathways, namely preloading and postloading. The former method uses template particles containing the substances of interest, followed by the assembly of a multilayered polymer film. The latter technique exploits a temporary change in the capsule permeability in response to external conditions (temperature, pH, light, etc.), which allows the loading of cargo in the capsule. In both cases, a key factor governing the success of encapsulation is the size of the encapsulated molecule. Globular proteins can be readily encapsulated in capsules using a range of compositions [41,42]. DNA, a natural polymer with a high molecular weight, has also been encapsulated into a number of multilayered capsular carriers [38,43]. Another important factor to consider for encapsulation is the charge-controlled permeability of the capsules. This technique utilizes the electrostatic repulsion between the cargo and the like-charged capsule membrane to suppress the outflow of encapsulated molecules [44]. The walls of the single-component disulfide-stabilized PMA capsules consist of a highly charged hydrogel, thus providing an effective barrier against the diffusion of like-charged encapsulated DNA molecules and allowing the permeation of the non-charged PVPON [38]. For this study, the oligopeptide of interest is KP9, a nine amino acid sequence which possesses a relatively low molecular weight (~1 kDa). It lacks substantial charge, and can freely diffuse through the walls of the PMA capsules. To achieve encapsulation of KP9 into PMA capsules, we propose a method of conjugation of the oligopeptide molecules to a negatively charged carrier polymer (Scheme 1) to take advantage of both factors that govern the permeability of multilayered capsules, namely steric hindrance and charge repulsion.

3.1. Preparation of the PMA–KP9 conjugate

The carrier (conjugate) polymer of choice was a 15 kDa sample of PMA, the same polymer used for the creation of the multilayered polymer capsules. This provides similar ionization behavior between the carriers and the capsule walls, achieving the encapsulation of small peptides. To manipulate the release of oligopeptides from the capsules, the conjugation of peptide to the carrier was achieved via a degradable disulfide linkage. In nature, the thiol-disulfide interconversions facilitate the maintenance of the tertiary structure of proteins in cells and play an important role in maintaining the extra- and intracellular redox potential. Within live cells, the content of reduced glutathione (GSH), a thiol-containing tripeptide, is generally higher than in the extracellular environment. This makes it possible to take advantage of thiol-disulfide chemistry for the creation of drug delivery vehicles that can be degraded upon cellular internalization [45]. Both the pristine form of PMA and KP9 are thiol-free molecules. In order for these molecules to form a disulfide linkage, we used an *N*-cysteine-modified KP9 (Cys-KP9) sequence and a thiol-modified PMA. The polymer was engineered to carry activated thiol groups to facilitate the formation of disulfide linkages with the oligopeptide via thiol-disulfide exchange (Scheme 2).

PMA was treated with cystamine in the presence of the carboxyl activating reagents EDC/NHS to obtain 5 mol% of thiol groups on the polymer. The thiolated polymer was then reduced by sodium borohydride and treated with 5,5′-dithiobis-2-nitrobenzoic acid (Ellman's reagent) to form a mixed disulfide (Scheme 2). The resulting polymer had a characteristic adsorption maximum at 335 nm (Fig. 1, spectrum A), which indicates the presence of activated thiol groups on the polymer. In this form, the thiol groups are protected from air oxidation and are activated towards the thiol-disulfide exchange. The conjugation of Cys-KP9 to the activated PMA_{SH} (denoted as PMA_{ER}) was conducted in Tris–EDTA buffer (pH 7.5) and was monitored by the release of a 2-nitro-5-mercaptobenzoic acid (TNB) chromophore with an absorbance maximum at 412 nm. Dithiothreitol (DTT) was used to ascertain the absorbance achieved upon the release of all TNB anions (Fig. 1, spectrum D), i.e. at full conversion of the conjugation reaction. Addition of the thiolated oligopeptide to a solution of PMA_{ER} resulted in an increase in absorbance at 412 nm (Fig. 1, spectra B and C), and in each case the reaction came to completion within 2 h (data not

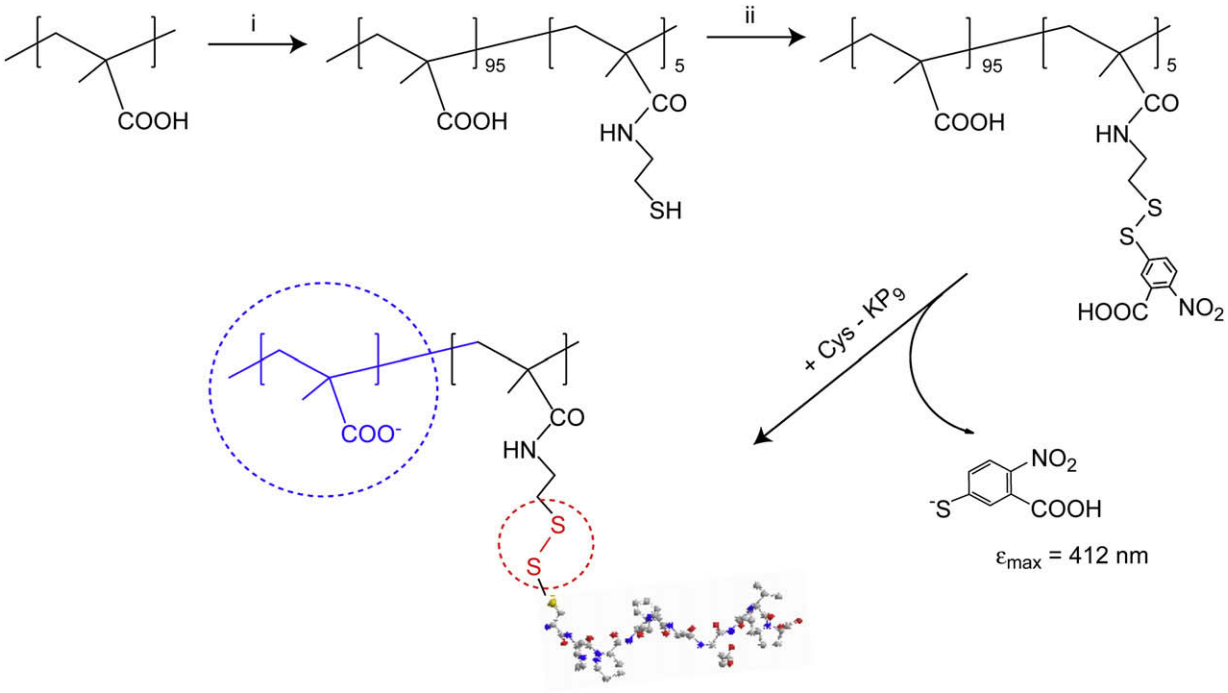

Scheme 2. Confinement of KP9 within polymer capsules through conjugating the oligopeptide to a carrier polymer. To achieve this, a sample of PMA was modified with thiol groups (i), which were subsequently activated for thiol-disulfide exchange using Ellman's reagent (ii). The resulting polymer was reacted with an *N*-terminal cysteine-modified KP9 to yield a PMA–KP9 conjugate wherein the PMA serves as an anchor for successful encapsulation. The disulfide linkage ensures a reversible nature of the linkage.

shown). The conjugation reaction was found to be near quantitative: at a 1:1 ratio of the thiol groups, Cys-KP9 led to almost complete release of TNB from PMA_{ER} (Fig. 1, spectrum C). The latter feature provides control over the degree of substitution on the polymer via the starting peptide to polymer concentration ratio.

3.2. Adsorption of the PMA–KP9 conjugate onto particles

The encapsulation of the polymer–peptide conjugate into multilayered polymer capsules was achieved via a procedure adopted from our previous reports on the encapsulation of gene vaccines [38]. Through this strategy we exploited amine-functionalized silica particles as templates to adsorb the PMA–KP9 conjugate, which then served as a support to assemble the multilayered polymer thin film. To quantify the adsorption of the PMA–KP9 conjugate on the template particles and facilitate visualization of encapsulated therapeutics, we used a Cys-KP9 oligopeptide bearing a fluorescent label (HiLyte Fluor 488) at the Cys end of the molecule in all experiments.

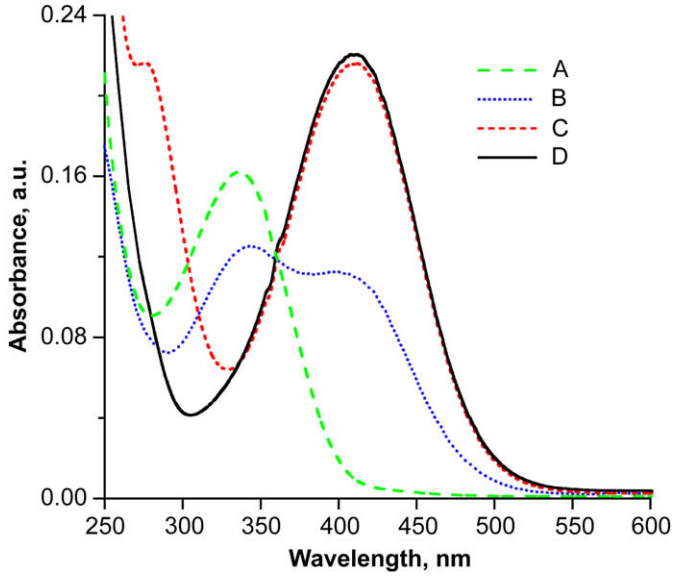

Fig. 1. UV–vis spectra of aqueous solutions of PMA_{ER} (A), solutions of mixtures of PMA_{ER} with Cys-KP9 at a molar ratio of polymer:peptide of 2:1 (B) and 1:1 (C) and excess DTT (D).

Solutions of varying concentration of the PMA–KP9 conjugate were incubated with 1 μm diameter SiO_2^+ particles at pH 7.5 and the fluorescence of the particles was quantified by flow cytometry (Fig. 2). Below saturation, the fluorescence of the particles increased linearly with increasing concentration of the conjugate and the fluorescence of the supernatants remained negligible, indicating that within the detection limits of the assay, all of the introduced conjugate was adsorbed onto the surface of the particles. The fluorescence of the particles reached a plateau at a surface coverage of ~0.8 mg m^{-2}. This value showed some batch-to-batch variation when different amine-functionalized silica samples or substitution degrees of PMA carriers were used. It should also be noted that when adsorption was conducted at lower pH the solubility of the PMA–KP9 conjugate decreased and caused a markedly higher adsorption of the conjugate onto the particles, leading to aggregation and poor control over the amount of conjugate adsorbed. Therefore, in all further experiments, the conjugate was adsorbed onto the particles from pH 7.5 Tris–EDTA buffer.

3.3. Capsule formation

The particles with immobilized PMA–KP9 were used as templates to assemble multilayered thin polymer films via the sequential adsorption of PMA_{SH} (12 mol% of thiol groups) and PVPON (Scheme 1). The process was initiated by the deposition of PVPON. All of the consecutive adsorption steps were conducted

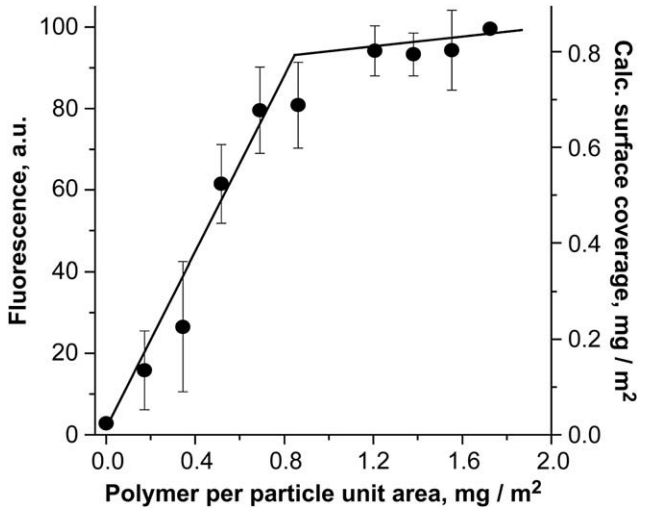

Fig. 2. Adsorption isotherm of the PMA–KP9 conjugate onto 1 μm diameter amine-functionalized silica particles from pH 7.5 Tris–EDTA buffer. The lines are to guide the eye only.

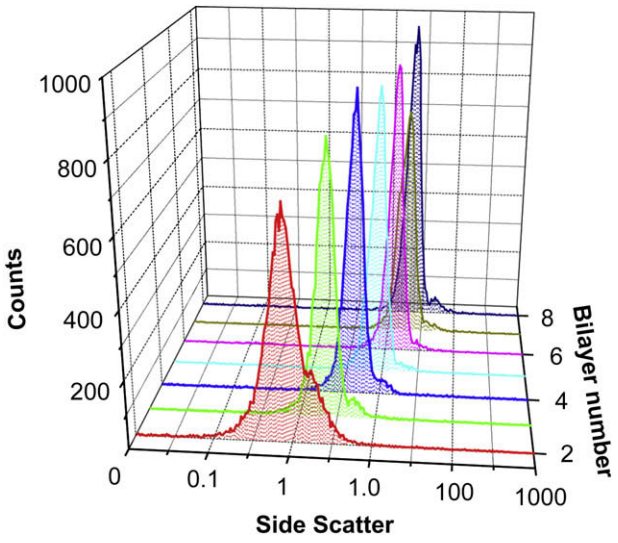

Fig. 3. Light scattering histograms for the 1 μm diameter disulfide cross-linked PMA/PVPON capsules with a different number of deposited polymer bilayers. The histograms were obtained using flow cytometry (side scatter) and pH 4 sodium acetate buffer and show a gradual increase in the amount of scattered light with the number of deposited polymer bilayers, which is indicative of the incremental increase in the thickness of the capsule wall.

from 1 g L^{-1} polymer solutions in 20 mM sodium acetate buffer, pH 4. We have previously shown that the encapsulation of DNA via a similar approach does not permit the use of template particles with over 50% coverage of the surface with a nucleic acid [38]. With increased surface coverage, the multilayer assembly became inefficient and yielded unstable capsules upon removal of the template silica core. However, the encapsulation of PMA–KP9 presented no restriction of this kind: the 1 μm template particles saturated with the conjugate successfully produce stable capsules upon cross-linking the PMA_{SH} thiol groups with chloramine T and removal of the template particles with aqueous hydrofluoric acid. With an increasing number of deposited bilayers, the capsules exhibited an increase in the intensity of scattered light, as monitored via flow cytometry (Fig. 3). This demonstrates an incremental growth in the thickness of the polymer film. The scattering histograms demonstrate that the capsules exhibited no tendency to aggregate, regardless of the number of deposited layers. This observation is important as particle flocculation is a limiting factor in the creation of colloidal gene/drug carriers. At pH 4, two bilayers of PVPON/PMA_{SH} deposited on top of the underlying PMA–KP9 conjugate were sufficient to produce stable capsules. These capsules exhibited structural integrity; that is, they could be spun down for purification purposes or buffer exchange, and remained stable over extended periods of time with no sign of degradation. However, these capsules were ineffective in retaining the cargo when transferred into pH 7.4 PBS (see below).

To investigate the efficiency of the PMA capsules to encapsulate the PMA–KP9 conjugate, template SiO_2^+ particles were used to adsorb fluorescently-labeled PMA (the carrier polymer used to anchor the peptides within the capsules). The PMA-coated particles were further coated with PVPON/PMA_{SH} layers. After each deposited bilayer, an aliquot of particles was extracted and the thiol groups on the PMA_{SH} layers were cross-linked with chloramine T to form disulfide linkages. The template particles were removed using HF, and the resulting capsules were washed into PBS, pH 7.4. At this pH, the hydrogen bonding between PMA_{SH} and PVPON is disrupted due to ionization of the PMA carboxyl groups. As a result, PVPON is released from the capsules [34], resulting in single-component PMA hydrogel capsules that are stabilized with disulfide linkages. The fluorescence of the resulting capsules was then quantified using flow cytometry (Fig. 4).

Upon removal of the template particles, the carrier polymer that was initially deposited onto the SiO_2^+ particles becomes the innermost layer of the capsule wall. Upon transfer into a buffer of $pH > pK_a$ (PMA) = 6.5, the carrier polymer separated from the capsule wall, relocating to the interior of the capsule due to electrostatic repulsion. Whilst the osmotic pressure of the encapsulated polymer provides a driving force for escape of the cargo into the bulk solution, it is counteracted by the steric and electrostatic

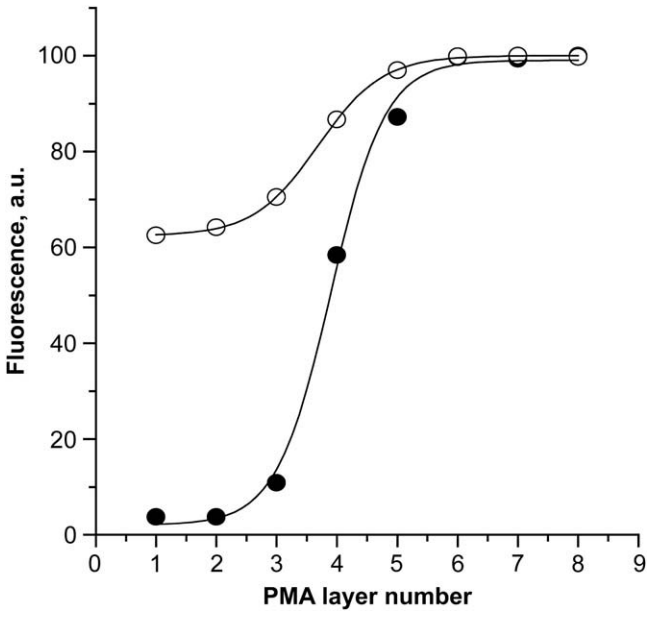

Fig. 4. Encapsulation efficiency (fluorescence of the encapsulated cargo associated with the capsule) exhibited by the 1 μm diameter disulfide cross-linked PMA capsules toward fluorescently-labeled 15 KDa PMA (closed circles) and PMA–KP9 conjugate (open circles) as a function of the number of PMA layers within the capsule wall. Retention of PMA (closed circles) is achieved via encapsulation into the interior of the capsules. For PMA–KP9 (open circles), the conjugate contained residual thiol groups which allows retention of the PMA–KP9 via both encapsulation into the capsule and covalent attachment to the capsule wall via a disulfide linkage.

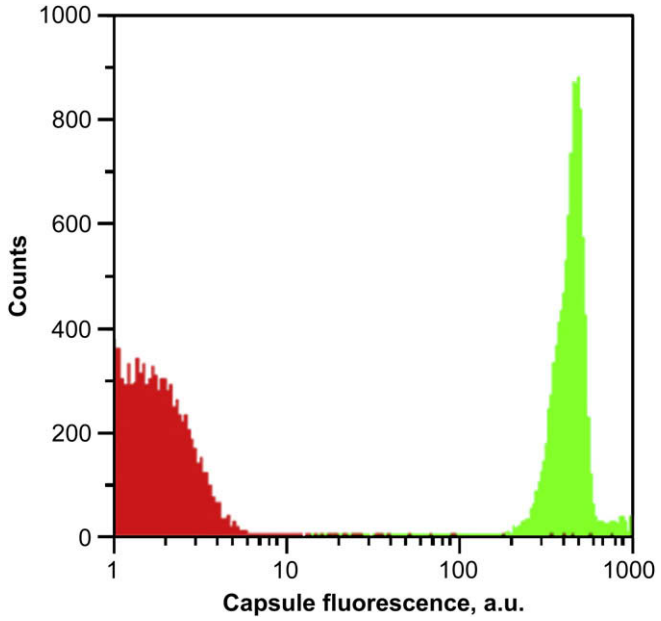

Fig. 5. Fluorescence intensity histogram obtained for the 1 μm diameter PMA capsules (5 layers of PMA). Fluorescently-labeled oligopeptides encapsulated in their pristine non-conjugated form (red) and as a conjugate with a carrier polymer, PMA (green).

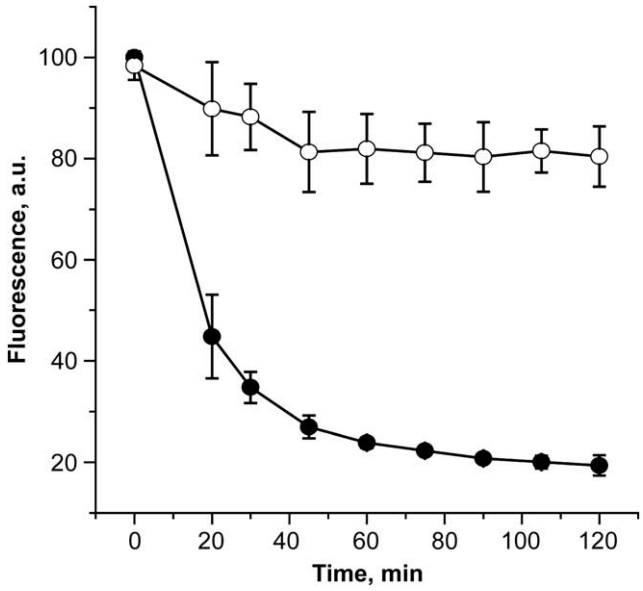

Fig. 7. Fluorescence of the 1 μm diameter KP9-loaded PMA hydrogel capsules (5 layers of PMA) in the presence of 5 mM GSH (closed circles) and GSSG (open circles). The fluorescent tag is covalently attached to the Cys-KP9. The decrease in fluorescence indicates release of the peptides from the capsules.

barrier created by the capsule walls, and the balance of these forces determines the effectiveness of encapsulation. With a low number of deposited layers the structurally intact capsules do not appear to provide any hindrance to the diffusion of the polymer-carrier and hence the capsules exhibited negligible fluorescence (Fig. 4). With an increasing number of deposited layers, the thickness of the PMA cross-linked hydrogel membrane *and* the electrostatic repulsion are increased, which results in a corresponding increase in the fluorescence of the capsule, indicating a greater amount of cargo payload is retained. Capsules composed of 6 or more layers of PMA retained all (within the limits of resolution of the fluorescence measurements) of the encapsulated 15 kDa PMA. We expect that the encapsulation efficiency profile will differ for species with different molecular weights and charge, and may also depend on other macromolecular characteristics such as the degree of branching and chain rigidity.

The incorporation of therapeutics into the PMA capsules can also be achieved via the covalent attachment of cargo to the capsule walls. To demonstrate this, we synthesized a sample of the PMA–KP9 conjugate with an incomplete conversion of PMA_{ER} thiols into oligopeptide-linked disulfides. The remaining thiol groups allowed

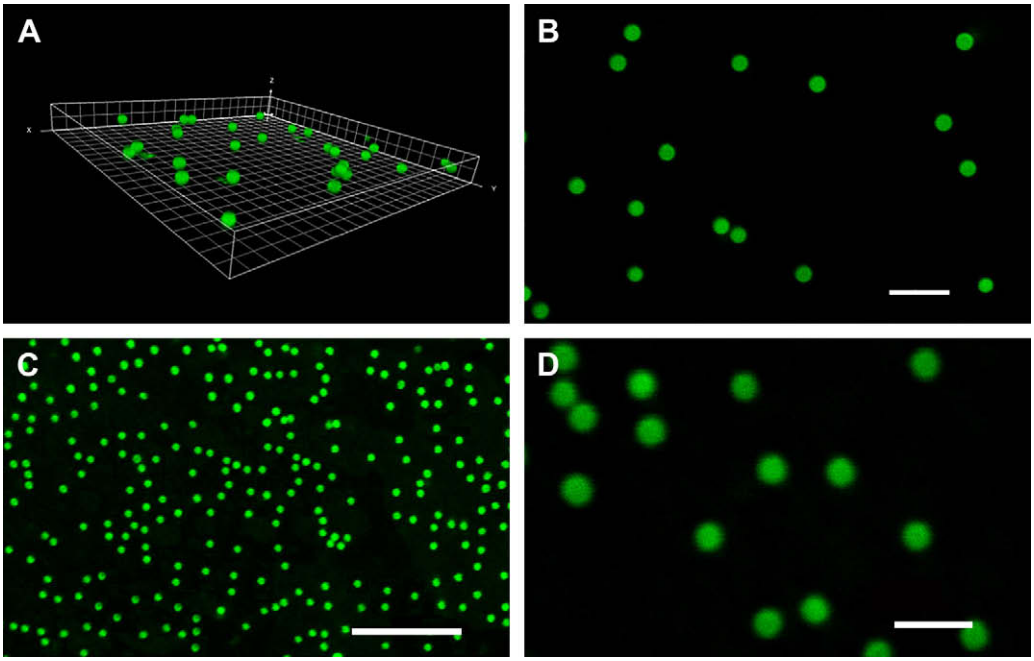

Fig. 6. CLSM images of the fluorescently-labeled PMA–KP9 conjugate encapsulated within 1 μm (A and B) and 0.5 μm (C and D) diameter PMA capsules. Scale bars are 5 μm (B and C) and 2 μm (D).

the conjugate to be covalently linked into the PMA capsule walls. In this case, even the capsules with the lowest number of deposited layers had a substantial amount of associated fluorescently-labeled oligopeptides (Fig. 4), making the capsules with as low as 2 layers of PMA suitable to serve as drug carriers. Notably, the encapsulation efficiency for a fraction of PMA–KP9 that was not linked into the capsule wall (ca. 40% in the presented case) followed the trends discussed above for the encapsulation of PMA.

In the above, we have outlined two strategies for the incorporation of polymer-bound oligopeptides into single-component PMA capsules, namely encapsulation of the payload into the interior of the capsules and incorporation of the cargo into the capsule walls. In practice, the two approaches most likely co-exist and contribute towards successful association of the oligopeptide with the carrier vehicle. In either case, the process required the conjugation of KP9 to a carrier polymer, while non-conjugated Cys-KP9 could not be encapsulated and was released even from the capsules with the highest number of layers examined (Fig. 5).

Confocal laser scanning microscopy (CLSM) was used to visualize the PMA–KP9 conjugate encapsulated into both 0.5 and 1 μm PMA capsules. The images show colloidally stable capsules that are monodisperse in size and uniformly loaded with the cargo (Fig. 6), in agreement with the flow cytometry data presented above. Using a combination of fluorescence spectroscopy (for quantification of the peptides) and flow cytometry (for absolute capsule counting), the oligopeptide loading in the capsules was calculated as 3×10^5 and 5×10^4 copies for 1 μm- and 0.5 μm-diameter capsules, respectively. The capsule loading was effectively controlled via the surface coverage of the template particle with the PMA–KP9 conjugate (see Fig. S1).

3.4. Release of KP9 in a reductive environment

The above data demonstrates the encapsulation of polymer-bound oligopeptides, KP9, within the confines of degradable polymer capsules. Conjugation of the oligopeptides to the carrier polymer is achieved via biodegradable disulfide linkages. Hence, once the capsules are internalized by cells, the intracellular reducing environment is expected to result in cleavage of these disulfide linkages. To mimic this process *ex vivo*, the fluorescently-labeled KP9-loaded capsules were incubated in PBS, pH 7.4 in the presence of 5 mM [46–48] reduced glutathione (Fig. 7). We have previously shown that under these conditions the disulfide-stabilized PMA capsules disintegrate over ~4 h of incubation [36]. The data in Fig. 7 indicate that release of KP9 occurs prior to complete degradation of the capsules. Within the first 20 min of incubation, the capsules demonstrated a 50% decrease in fluorescence of the cargo, and by 1 h about 80% of the cargo had been released. The minor initial release of KP9 in response to the oxidized, dimeric form of glutathione, GSSG, was similar to that of the samples incubated in serum (data not shown), and may be attributed to a slight change in the permeability of the capsules in response to the external conditions.

3.5. Immunostimulatory activity of capsule cargo

For successful application, the methods used for the conjugation of peptides/drugs to macromolecular carriers and/or encapsulation of the therapeutic molecules into supramolecular vehicles need to be non-degrading and non-damaging to the cargo to ensure the released therapeutics retain their biological activity. To test this for

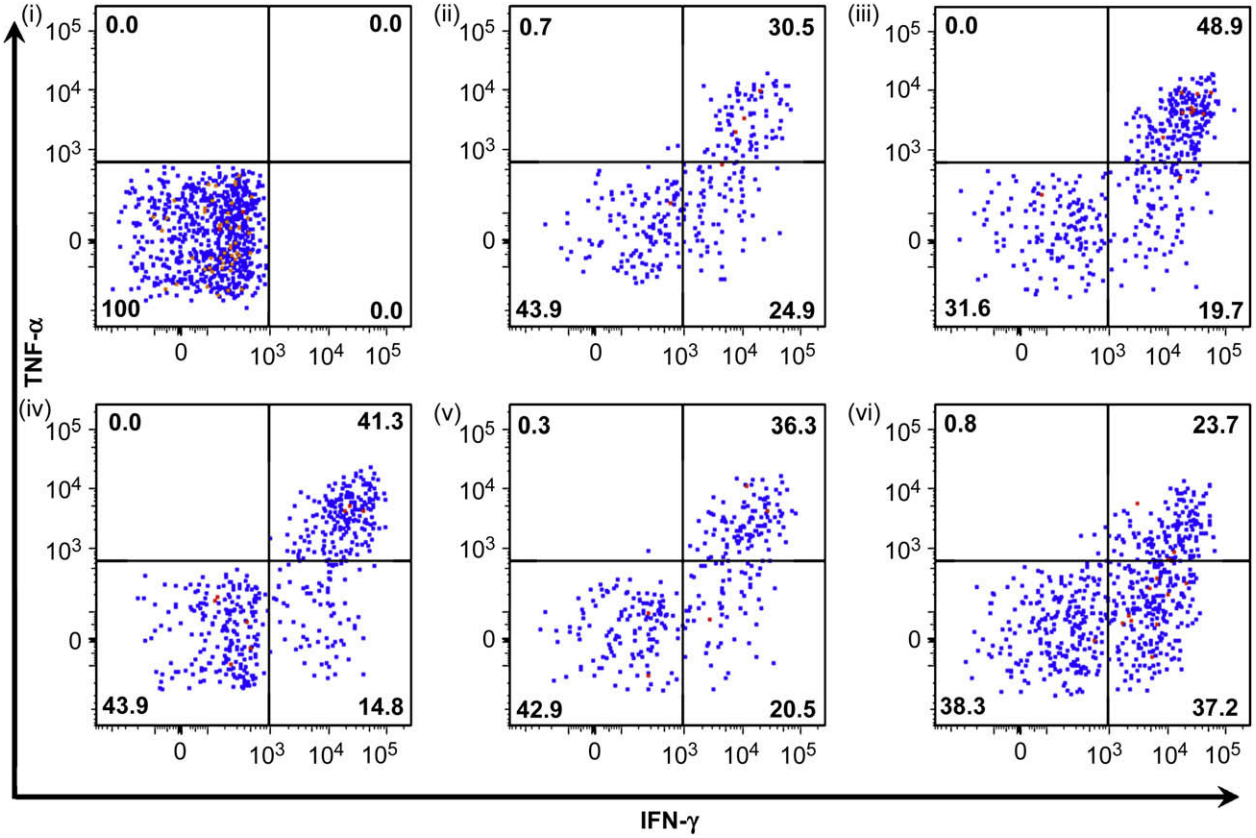

Fig. 8. Immunostimulatory capacity of KP9 preparations. Macaque blood was incubated with various KP9 preparations and KP9-specific T cells assessed for intracellular IFN-γ and TNF-α expression: (i) unstimulated; (ii) KP9 peptide (0.1 μg); (iii) Cys-KP9 (0.1 μg); (iv) conjugate (Cys-KP9 + PMA_{ER}) (0.1 μg); (v) GSH treated Cys-KP9 (0.1 μg); (vi) GSH treated KP9-loaded capsules of 0.5 μm diameter (equivalent to 0.1 μg Cys-KP9).

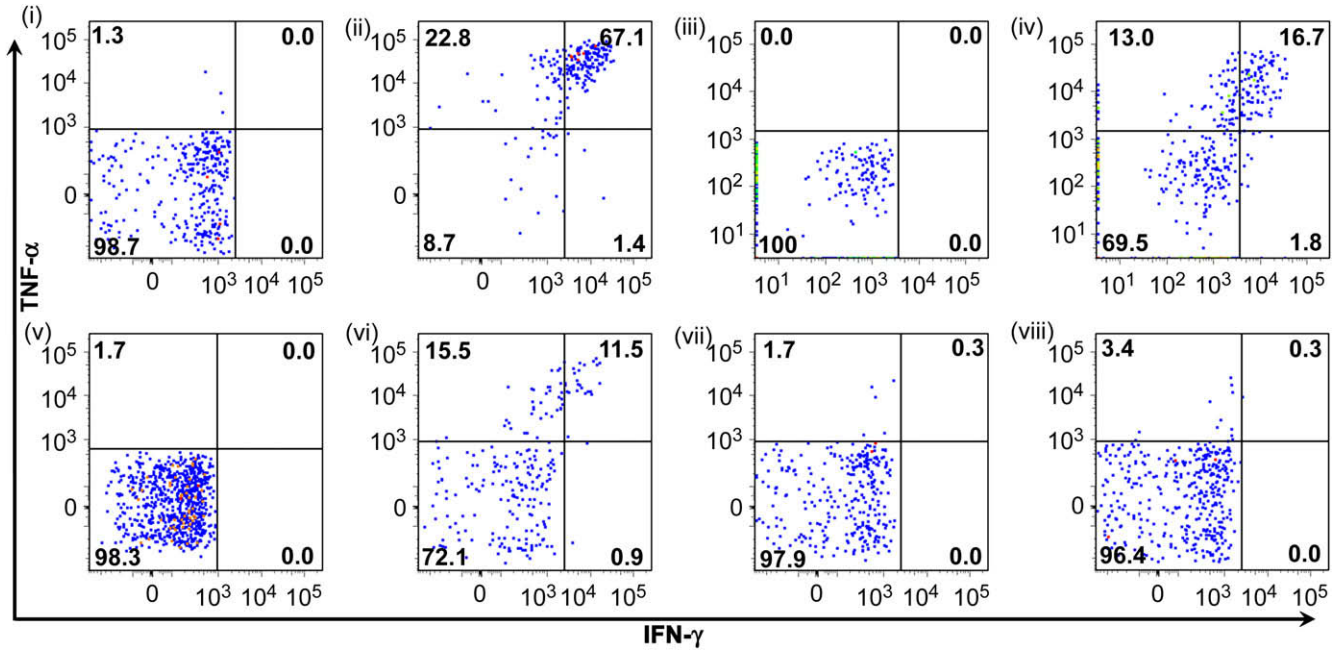

Fig. 9. Immunostimulatory capability of KP9-loaded capsules: (i) unstimulated; (ii) Cys-KP9 (0.1 μg); (iii) 0.5 μm empty capsules (1000 capsules: 1 leukocyte); (iv) 0.5 μm KP9-loaded capsules (100:1); (v) 1 μm empty (CpG) capsules (50:1); (vi) 1 μm KP9-loaded capsules (50:1); (vii) supernatant (50:1); (viii) supernatant (500:1).

the PMA–KP9 conjugate, we made use of a non-human primate model of SIV infection. The KP9 peptide is an epitope from the SIV protein Gag, which is known to be presented on the surface of antigen presenting cells (APCs) as a complex with a particular major histocompatibility I (MHC-I) molecule, Mane-A*10 [49]. In SIV infected pigtail macaques, presentation of this KP9-MHC-I complex on the surface of APCs is recognized by circulating KP9-specific CD8 T cells that will become reactivated and produce cytokines (such as interferon-γ (IFN-γ) and the tumor necrosis factor-α (TNF-α)) in response to this presentation [50]. The KP9-specific T cells were identified by flow cytometry using a fluorescent Mane-A*10/KP9 tetramer molecule and the activation of this defined cell population in response to KP9 was investigated by staining for intracellular expression of the cytokines IFN-γ and TNF-α from whole blood taken from these macaques. In the absence of stimulation with the KP9 peptide, the circulating KP9-specific T cells were not activated and thus did not produce cytokines (Fig. 8i). Upon addition of free KP9 to blood, the soluble peptide bound directly to the MHC-I on the surface of the APCs in the blood and activated the cognate T cells. Hence a large proportion of the KP9-specific T cells were activated to produce both IFN-γ and TNF-α (Fig. 8ii). These two experiments provided a negative and a positive control, respectively. The addition of fluorescently-labeled Cys-KP9 (Fig. 8iii) as well as the conjugate of Cys-KP9 with PMA used in the encapsulation (Fig. 8iv) also led to T cell activation, indicating that chemical modification of pristine KP9 did not prevent the processing of the MHC-I/KP9 complex and subsequent activation of the specific T cells. In the presence of 5 mM GSH, that is, upon degradation of the disulfide bonds, the Cys-KP9 retained its ability to activate the corresponding T cells (Fig. 8v). Furthermore, the use of the lysate obtained via GSH treatment of capsules with encapsulated PMA–KP9 also led to T cell activation (Fig. 8vi). These data substantiate that chemical modification of the KP9 peptide did not impair the ability of this peptide to stimulate T cell immunity.

The immunostimulatory capabilities of intact capsules were then investigated using the same assay system. In order for the encapsulated Cys-KP9 to activate KP9-specific T cells, the PMA capsules must be internalized by APCs to result in degradation of the capsules under the reducing environment inside the cell, releasing the Cys-KP9 from the capsules and carrier polymer, to allow binding to MHC-I, transportation to the cell surface, and presentation to cognate T cells. Flow cytometry and confocal microscopy have previously confirmed that PMA capsules are internalized by fresh human APCs [35]. Capsules with a diameter of 0.5 and 1 μm demonstrated KP9-specific T cell activation upon incubation with macaque blood (Fig. 9, panels iv and vi). Empty capsules which did not contain any peptide did not activate the KP9-specific T cells (Fig. 9, panels iii and v), demonstrating that the T cell activation induced was due to the KP9 within the capsules and not due to any immunostimulatory effects of the capsules themselves. The supernatant from the capsules did not result in KP9-specific T cell activation (Fig. 9, panels vii and viii), substantiating that the T cell activation was due to intracellular processing of the KP9 rather than leakage of the peptide from the capsules. This indicates that the biologically active cargo is retained within the capsules until intracellular degradation occurs and the KP9 peptide is processed by the APCs to elicit an immune response.

4. Conclusion

This paper presents a novel vaccine approach based on the delivery of viral protein epitopes to antigen presenting cells within degradable polymer capsules. This is achieved by an all-aqueous procedure for the conjugation and encapsulation of oligopeptides within micron and submicron sized polymer capsules. Our system provides control over the size of the delivery vehicle and loading of the peptide vaccine. The cargo therapeutic is confined within the capsules in physiological conditions and is released within human cells in the presence of a natural reducing agent, glutathione. Upon release from the capsules, the oligopeptide retains its functional activity, and the intact capsules are successful in delivering their cargo vaccine to the APCs to re-stimulate specific T cells. Taken together, these data represent a novel paradigm in vaccine delivery which holds promise for vaccination, drug delivery and other biomedical applications.

Acknowledgements

This research was supported by the Australian Research Council grants under the Federation Fellowship (FC) and Discovery Project (FC, ANZ) schemes, National Health and Medical Research Council grants (SJK), and the University of Melbourne Strategic Research Infrastructure Fund (FC, SJK).

Appendix

Figures with essential colour discrimination. The majority of figures in this article, have parts that may be difficult to interpret in black and white. The full colour images can be found in the on-line version, at doi:10.1016/j.biomaterials.2009.05.078.

Appendix. Supplementary data

Supplementary data associated with this article can be found in the on-line version at doi:10.1016/j.biomaterials.2009.05.078.

References

[1] Boyle JS, Brady JL, Lew AM. Enhanced responses to a DNA vaccine encoding a fusion antigen that is directed to sites of immune induction. Nature 1998;392:408–11.
[2] Lu W, Wu X, Lu Y, Guo W, Andrieu JM. Therapeutic dendritic-cell vaccine for simian AIDS. Nat Med 2003;9:27–32.
[3] Hawkins OE, Van Gundy RS, Eckerd AM, Bardet W, Buchli R, Weidanz JA, et al. Identification of breast cancer peptide epitopes presented by HLA-A*0201. J Proteome Res 2008;7:1445–57.
[4] Jung HH, Yi HJ, Lee SK, Lee JY, Jung HJ, Yang ST, et al. Structural analysis of immunotherapeutic peptides for autoimmune myasthenia gravis. Biochemistry 2007;46:14987–95.
[5] Manea M, Hudecz F, Przybylski M, Mezõ G. Synthesis, solution conformation, and antibody recognition of oligotuftsin-based conjugates containing a β-amyloid(4-10) plaque-specific epitope. Bioconjugate Chem 2005;16:921–8.
[6] Chea S, Dale CJ, De Rose R, Ramshaw IA, Kent SJ. Enhanced cellular immunity in macaques following a novel peptide immunotherapy. J Virol 2005;79:3748–57.
[7] Neundorf I, Rennert R, Franke J, Közle I, Bergmann R. Detailed analysis concerning the biodistribution and metabolism of human calcitonin-derived cell-penetrating peptides. Bioconjugate Chem 2008;19:1596–603.
[8] Putnam D. Polymers for gene delivery across length scales. Nat Mater 2006;5:439–51.
[9] Duncan R. The dawning era of polymer therapeutics. Nat Rev Drug Disc 2003;2:347–60.
[10] Edwards DA, Hanes J, Caponetti G, Hrkach J, Ben-Jebria A, Eskew ML, et al. Large porous particles for pulmonary drug delivery. Science 1997;276:1868–71.
[11] Torchilin VP. Recent advances with liposomes as pharmaceutical carriers. Nat Rev Drug Disc 2005;4:145–60.
[12] Gursoy RN, Benita S. Self-emulsifying drug delivery systems (SEDDS) for improved oral delivery of lipophilic drugs. Biomed Pharmacother 2004;58:173–82.
[13] Kataoka K, Harada A, Nagasaki Y. Block copolymer micelles for drug delivery: design, characterization and biological significance. Adv Drug Delivery Rev 2001;47:113–31.
[14] Quinn JF, Johnston APR, Such GK, Zelikin AN, Caruso F. Next generation, sequentially assembled ultrathin films: beyond electrostatics. Chem Soc Rev 2007;36:707–18.
[15] De Geest BG, Sanders NN, Sukhorukov GB, Demeester J, De Smedt SC. Release mechanisms for polyelectrolyte capsules. Chem Soc Rev 2007;36:636–49.
[16] Gittins DI, Caruso F. Multilayered polymer nanocapsules derived from gold nanoparticle templates. Adv Mater 2000;12:1947–9.
[17] Gittins DI, Caruso F. Tailoring the polyelectrolyte coating of metal nanoparticles. J Phys Chem B 2001;105:6846–52.
[18] Schneider G, Decher G. Functional core/shell nanoparticles via layer-by-layer assembly. Investigation of the experimental parameters for controlling particle aggregation and for enhancing dispersion stability. Langmuir 2008;24:1778–89.
[19] Caruso F. Nanoengineering of particle surfaces. Adv Mater 2001;13:11–22.
[20] Shenoy DB, Antipov AA, Sukhorukov GB, Möhwald H. Layer-by-layer engineering of biocompatible, decomposable core–shell structures. Biomacromolecules 2003;4:265–72.
[21] Saurer EM, Jewell CM, Kuchenreuther JM, Lynn D. Assembly of erodible, DNA-containing thin films on the surfaces of polymer microparticles: toward a layer-by-layer approach to the delivery of DNA to antigen-presenting cells. Acta Biomaterialia 2009;5:913–24.
[22] Glinel K, Déjugnat C, Prevot M, Schöler B, Schönhoff M, von Klitzing R. Responsive polyelectrolyte multilayers. Colloids Surf A 2007;303:3–13.
[23] Angelatos AS, Katagiri K, Caruso F. Bioinspired colloidal systems via layer-by-layer assembly. Soft Matter 2006;2:18–23.
[24] Angelatos AS, Radt B, Caruso F. Light-responsive gold nanoparticle polyelectrolyte/gold microcapsules. J Phys Chem B 2005;109:3071–6.
[25] Radt B, Smith T, Caruso F. Optically addressable nanostructured capsules. Adv Mater 2004;16:2184–9.
[26] Antipov AA, Sukhorukov GB. Polyelectrolyte multilayer capsules as vehicles with tunable permeability. Adv Col Inter Sci 2004;111:49–61.
[27] Zhao QH, Han BS, Wang ZH, Gao CY, Peng CH, Shen JC. Hollow chitosan–alginate multilayer microcapsules as drug delivery vehicle: doxorubicin loading and in vitro and in vivo studies. Nanomed Nanotechnol Biol Med 2007;3:63–74.
[28] Cortez C, Tomaskovic-Cook E, Johnston APR, Scott AM, Nice EC, Heath JK, et al. Influence of size, surface, cell line and kinetic properties on the specific binding of A33 antigen-targeted multilayered particles and capsules to colorectal cancer cells. ACS Nano 2007;1:93–102.
[29] Haložan D, Riebentanz U, Brumen M, Donath E. Polyelectrolyte microcapsules and coated $CaCO_3$ particles as fluorescence activated sensors in flowmetry. Colloids Surf A Physicochem Eng Aspects 2009;342:115–21.
[30] Johnston APR, Caruso F. A molecular beacon approach to measuring the DNA permeability of thin films. J Am Chem Soc 2005;127:10014–5.
[31] Dähne L, Leporatti S, Donath E, Möhwald H. Fabrication of micro reaction cages with tailored properties. J Am Chem Soc 2001;277:5431–6.
[32] Price AD, Zelikin AN, Wang Y, Caruso F. Triggered enzymatic degradation of DNA within selectively permeable polymer capsule microreactors. Angew Chem Int Ed 2009;48:329–32.
[33] Städler B, Chandrawati R, Price AD, Chong S-F, Breheney K, Postma A, et al. A microreactor with thousands of subcompartments: enzyme-loaded liposomes within polymer capsules. Angew Chem Int Ed 2009;48:4359–62.
[34] Zelikin AN, Li Q, Caruso F. Disulfide-stabilized poly(methacrylic acid) capsules: formation, cross-linking, and degradation behavior. Chem Mater 2008;20:2655–61.
[35] De Rose R, Zelikin AN, Johnston APR, Sexton A, Chong S-F, Cortez C, et al. Binding, internalization and antigen presentation of vaccine-loaded nano-engineered capsules in blood. Adv Mater 2008;20:4698–703.
[36] Zelikin AN, Quinn JF, Caruso F. Disulfide cross-linked polymer capsules: en route to biodeconstructible systems. Biomacromolecules 2006;7:27–30.
[37] Zelikin AN, Li Q, Caruso F. Degradable polyelectrolyte capsules filled with oligonucleotide sequences. Angew Chem 2006;118:7907–9.
[38] Zelikin AN, Becker AL, Johnston APR, Wark KL, Turatti F, Caruso F. A general approach for DNA encapsulation in degradable polymer microcapsules. ACS Nano 2007;1:63–9.
[39] Sivakumar S, Bansal V, Cortez C, Chong S-F, Zelikin AN, Caruso F. Degradable, surfactant-free, monodisperse polymer-encapsulated emulsions as anti-cancer drug carriers. Adv Mater 2009;21:1820–4.
[40] Werle M, Hoffer M. Glutathione and thiolated chitosan inhibit multidrug resistance P-glycoprotein activity in excised small intestine. J Controlled Release 2006;111:41–6.
[41] Wang Y, Caruso F. Enzyme encapsulation in nanoporous silica spheres. Chem Commun 2004;13:1528–9.
[42] Volodkin DV, Petrov AI, Prevot M, Sukhorukov GB. Matrix polyelectrolyte microcapsules: new system for macromolecule encapsulation. Langmuir 2004;20:3398–406.
[43] Kreft O, Georgieva R, Bäumler H, Steup M, Müller-Röber B, Sukhorukov GB, et al. Red blood cell templated polyelectrolyte capsules: a novel vehicle for the stable encapsulation of DNA and proteins. Macromol Rapid Commun 2006;27:435–40.
[44] Tong W, Dong W, Gao C, Möhwald H. Charge-controlled permeability of polyelectrolyte microcapsules. J Phys Chem B 2005;109:13159–65.
[45] Saito G, Swanson JA, Lee K-D. Drug delivery strategy utilizing conjugation via reversible disulfide linkages: role and site of cellular reducing activities. Adv Drug Deliv Rev 2003;55:199–215.
[46] Hwang C, Lodish HF, Sinskey AJ. Measurement of glutathione redox state in cytosol and secretory pathway of cultured-cells. Methods Enzymol 1995;251:212–21.
[47] Gilbert HF. Molecular and cellular aspects of thiol-disulfide exchange. Adv Enzymol 1990;63:69–172.
[48] Kosower NS, Kosower EM. The glutathione (GSH) status of cells. Int Rev Cytol 1978;54:109–60.
[49] Smith MZ, Dale CJ, De Rose R, Stratov I, Fernandez CS, Brooks AG, et al. Analysis of pigtail macaque major histocompatibility complex class I molecules presenting immunodominant simian immunodeficiency virus epitopes. J Virol 2005;79:684–95.
[50] Rollman E, Smith MZ, Brooks AG, Purcell DFJ, Zuber B, Ramshaw IA, et al. Killing kinetics of simian immunodeficiency virus-specific CD8(+) T cells: implications for HIV vaccine strategies. J Immunol 2007;179:4571–9.